Published in final edited form as:
Mol Ther. 2007 April ; 15(4): 705–712. doi:10.1038/mt.sj.6300106.

Spatially Patterned Gene Delivery for Localized Neuron Survival and Neurite Extension

Tiffany Houchin-Ray[1], **Kevin J Whittlesey**[2], and **Lonnie D Shea**[1,3,4]

1*Department of Chemical and Biological Engineering, Northwestern University, Evanston, Illinois, USA*

2*Interdepartmental Biological Sciences, Northwestern University, Evanston, Illinois, USA*

3*Department of Biomedical Engineering, Northwestern University, Evanston, Illinois, USA*

4*Institute for BioNanotechnology in Medicine, Northwestern University, Evanston, Illinois, USA*

Abstract

Natural tissues can have complex architectures, which arise in part from spatial patterns in gene expression. Regenerative strategies for damaged tissue must recreate these architectures to restore function. In this article, we demonstrate spatially controlled gene delivery from a substrate for directing cellular processes. Non-viral vectors were immobilized to substrates in linear patterns using microfluidic techniques, and cells cultured on the surface had localized gene expression within the cell population. Transfection was achieved in pattern widths as low as 100 μm, with efficiencies dependent on the microchannel treatment and vector concentration. The ability of patterned expression to localize cellular processes was investigated using a neuronal co-culture model. Patterned expression of the diffusible neurotrophic factor nerve growth factor initiated neuron survival and neurite outgrowth primarily within the pattern, which decreased significantly in regions directly adjacent to the pattern. Primary neurite density was significantly greater on patterned substrates than on surfaces without patterns. This approach demonstrates the basic technology to create patterns of gene expression that can direct tissue formation and could be employed in regenerative strategies to recreate the complex cellular architectures observed in tissues.

INTRODUCTION

Natural tissues can have complex architectures characterized by the organization of multiple cell types into structures, such as branching networks of the vascular or nervous systems. This cellular organization arises, in part, from spatial patterns in gene expression, which can create concentration gradients of diffusible factors that direct cellular processes. During morphogenesis, gradients of the sonic hedgehog,[1–3] transforming growth factor-β,[4–6] and Wingless[7–9] families of proteins direct cellular differentiation. Gradients of platelet-derived growth factor and basic fibroblast growth factor are chemotactic agents for dermal fibroblasts[10,11] and smooth muscle cells,[12] respectively. In addition, neurons have receptors for diffusible guidance factors such as netrins, semaphorins, and neurotrophic factors that induce and direct axonal elongation.[13–15] Engineering patterns of gene expression may provide a means to direct cellular processes (*e.g.*, cell migration, neurite extension) for the regeneration of tissues with complex architectures.

Correspondence: Lonnie D Shea, Department of Chemical and Biological Engineering, Northwestern University, 2145 Sheridan Road/ E156, Evanston, Illinois 60208-3120, USA. E-mail: l-shea@northwestern.edu.

Gene delivery from biomaterial scaffolds for tissue engineering offers the potential to support and direct progenitor cell differentiation and migration into functional tissue replacements. Biomaterials play a central role in the engineering of tissue replacements and are designed to present a combination of insoluble and soluble signals that promote tissue formation.[16–18] Gene delivery from a tissue engineering scaffold is a versatile approach to inducing expression of tissue inductive factors, with expression lasting for days to months.[19,20] Gene therapy vectors, either virus derived or non-viral (*i.e.*, synthetic), can be immobilized to tissue culture substrates through either specific (*e.g.*, biotin–avidin) or nonspecific (*e.g.*, electrostatic, van der Waals) interactions.[21–23] This technique, termed substrate-mediated gene delivery or reverse transfection, places complexes directly in the cellular microenvironment for efficient internalization, and high transfection efficiencies can be achieved with less DNA than in traditional bolus delivery.[24,25] In addition, the immobilization of gene therapy vectors provides the means to restrict complex deposition spatially and potentially to pattern gene expression. Patterned gene expression may offer significant advantages over protein patterning, which has been widely used to pattern cellular responses.[26–31]

In this article, we describe a system to pattern non-viral DNA complexes spatially on a cell adhesive substrate to promote cellular processes within the pattern. Polydimethylsiloxane (PDMS) microchannels were used to pattern the nonspecific immobilization of cationic lipid/DNA complexes, termed lipoplexes, onto tissue culture polystyrene (TCPS). Treatments were investigated to minimize the interactions between the lipoplexes and PDMS, particularly given the relatively high microchannel volume to TCPS surface area ratio. Polydimethylsiloxane microchannels (100–1,000 μm widths) were treated by either O_2 plasma exposure or soaking in a Pluronic L35 solution (hereafter referred to as Pluronic) to render the microchannels hydrophilic and reduce adsorption of the lipoplexes to PDMS. The microchannel treatments were investigated to achieve efficient and patterned complex binding to the surface, while maintaining complex activity for efficient and patterned transfection. Parameters such as microchannel dimensions and treatment and vector concentration were varied to achieve high transfection efficiency. The patterned expression system was investigated for the ability to localize cellular processes using a neuronal co-culture model. Neuron survival and neurite outgrowth were assessed within patterns, and at specific distances outside patterns, of neurotrophic factor expression. This system provides a platform with which to investigate patterns of gene expression in tissue formation, and could be applied for the engineering of functional tissue replacements.

RESULTS AND DISCUSSION

Patterned lipoplex deposition and binding

Lipoplexes were deposited on TCPS surfaces using microfluidic devices fabricated by soft lithography. This technique is commonly used to fabricate PDMS microchannels for the patterned deposition of protein or cellular adhesion, but it has never been utilized to pattern DNA complexes.[32,33] Polydimethylsiloxane is hydrophobic and strongly adsorbs a range of macromolecules; thus, PDMS is commonly treated to render it hydrophilic and reduce adsorption.[34] In these studies, O_2 plasma and Pluronic treatments were investigated for their effects on patterned deposition and complex binding. Incubation of lipoplexes within Pluronic-treated PDMS microchannels produced patterns of deposition in widths of 1,000 μm (Figure 1a), 500 μm (Figure 1b), 250 μm (Figure 1c), and 100 μm (Figure 1d). The width of the pattern matched the width of the microchannel. Pluronic treatment of the channels produced a more dense and homogeneous layer of deposited lipoplexes in a 1,000 μm wide pattern (Figure 1a) as compared with lipoplexes incubated in untreated channels (Figure 1e).

The binding efficiency, defined as the amount of DNA bound divided by the amount incubated in the microchannel, was dependent on the channel width and treatment. Higher binding

efficiencies were observed with O_2 plasma- and Pluronic-treated microchannels than with untreated microchannels (Figure 2a, $P < 0.05$). O_2 plasma and Pluronic treatments increased the binding efficiency to 23%, compared with 15% with no treatment, presumably by decreasing interactions between PDMS and lipoplexes. O_2 plasma exposure introduces silanol groups on the PDMS surface at the expense of methyl groups, but the hydrophilic surface is unstable in ambient air.[34,35] Pluronic, a block co-polymer of poly(ethylene oxide)-poly (propylene oxide)-poly(ethylene oxide), can anchor to a hydrophobic solid surface, such as PDMS, through interactions with the hydrophobic poly(propylene oxide) block.[36] In addition, the binding efficiency decreased as the channel width decreased (Figure 2b, $P < 0.05$). Decreasing the width of the Pluronic-treated PDMS microchannel decreased the binding efficiency, from 23% for a 1,000 μm channel to 3% for a 100 μm channel. The microchannel volume to TCPS surface area ratio increases with decreasing microchannel width, and normalization of the binding efficiency to the relative PDMS surface area led to similar binding efficiencies for all channel widths (data not shown). Therefore, we conclude that an increase in PDMS surface area contributed to the decrease in binding efficiency, as the Pluronic treatment did not completely eliminate interactions between lipoplexes and PDMS.

Spatial patterns of gene expression

Pluronic-treated PDMS microchannels afforded the ability to deposit active lipoplexes and produced 1,000–100 μm wide patterns of transgene expression. Nonspecific immobilization of the lipoplexes resulted in localized gene expression (Figure 3a–h), with the dimensions of the patterned regions matching the microchannel dimensions. Nonspecific immobilization between lipoplexes and TCPS results in approximately 10% complex release in cell culture medium after 24 hours.[24] The correlation between immobilization (Figure 1) and transfection (Figure 3) observed here may result from either (i) lipoplexes internalized directly from the surface or (ii) lipoplexes released from the surface that primarily associate with cells in the pattern, with escaping lipoplexes becoming diluted and thus ineffective.

The treatment of the microchannel before complex deposition was critical to transfecting HEK293T cells cultured on the substrate. Transfection was observed with lipoplexes deposited using Pluronic-treated microchannels, but no transfection was observed with untreated or O_2 plasma-treated microchannels (data not shown). Pluronic mixed with cationic polymers or lipids can increase transfection efficiency compared with polymer or lipid alone.[37–39] Here, loosely bound Pluronic may interact with the lipoplexes to prevent complex aggregation or enhance complex association with the cells. Pluronic may also influence the nonspecific interactions between the lipoplex and substrate. By adsorbing to TCPS, Pluronic may modulate the surface chemistry and thus influence the binding affinity between the complexes and the surface, which in turn affects transfection efficiency.[40]

The vector concentration influenced transfection efficiency in patterns of all sizes. Relatively high transfection efficiencies (above 25%) were achieved using Pluronic-treated microchannels for all widths (Figure 4). However, high levels of transfection could be achieved in the smaller channel widths only by increasing the concentration of DNA. The decreasing binding efficiency within the narrower channel presumably leads to insufficient quantities on the surface. The vector concentrations in solution that produce the relatively high transfection efficiencies correspond to surface densities of approximately 0.01–0.03 μg DNA/cm^2 (Figure 2). Interestingly, these densities of immobilized lipoplexes were approximately 10-fold lower than that required to achieve comparable transfection efficiencies in tissue culture plates (*i.e.*, without microchannels) (0.2 μg DNA/cm^2),[24] further suggesting that Pluronic treatment may increase the delivery efficiency. The range of vector concentrations at which the relatively high transfection efficiency is achieved becomes narrower as the pattern width decreases (Figure 4). At high DNA concentrations, complex aggregation in small volumes may also

hinder transfection. For lipoplexes incubated in the 100 μm channel, increasing the vector concentration (from 10 to 50 ng/μl) increased the average lipoplex diameter on the surface (data not shown).

The use of microfluidic devices is a novel approach to patterning gene expression. Methods to localize DNA delivery have been developed previously, with specifically tethered viral vectors on polyurethane films[21] or mechanical spotting of non-viral vectors.[25] The microfluidics approach can produce complex patterns on a uniform substrate using PDMS microchannels in a range of sizes or shapes. Most important, the system can achieve these complex patterns with dimensions on the order of 100 μm, which is a size consistent with many cellular structures within tissues.

Localization of neuron survival and neurite extension

This method of spatially patterning gene expression was subsequently investigated for directing cellular processes using an *in vitro* neuronal co-culture model. Patterned transfection of the diffusible neurotrophic factor nerve growth factor (NGF) could lead to localized and sustained secretion. Previous efforts to localize neurite outgrowth have focused on the patterning of adhesion molecules (*e.g.*, extracellular matrix molecules) to guide cellular adhesion and neurite extension.[41–44] One challenge related to patterning proteins for guiding cellular processes is nonspecific adsorption of serum or cell-secreted proteins that can mask or displace the immobilized proteins. Gene delivery, in contrast, can sustain transgene expression for timescales ranging from days to months,[19] with the persistence of the factors maintaining a stimulus locally to promote the cellular process. We hypothesize that the patterned expression of neurotrophic factors provides the stimulus to promote neuron survival and neurite outgrowth, and also the directional cue to orient neurite extension.

Primary neurons and HEK293T cells were cultured on patterns (250, 100 μm) with immobilized lipoplexes that contained a 50:50 mix of plasmid encoding for nerve growth factor (pNGF) (to promote neurite outgrowth) and enhanced green fluorescent protein (pEGFP) (to visualize transfected cells). Vector concentrations were selected based on the lowest concentration to yield at least 30% transfection efficiency (250 μm: 8 ng/μl; 100 μm: 10 ng/μl). Patterns of NGF expression were sufficient to localize neuron survival and neurite outgrowth. Neurite extension and neuron survival were apparent directly within the area of patterned transfection for 250 μm (Figure 5a and b) and 100 μm (Figure 5c and d) wide patterns. The absence of pNGF, or cells transfected with an empty vector, did not support either neuron survival or neurite extension (data not shown). Since HEK293T cells did not basally support neuron survival, the behavior of dorsal root ganglia neurons in the co-culture system was directly attributed to the patterns of NGF expression.

Neuron survival and neurite density were assessed at the location of patterned NGF expression, and in 100 μm increments away from the pattern. Neuron survival (normalized to surface area) was comparable on patterns of 250 and 100 μm wide NGF expression (Figure 6a). Neuron survival decreased significantly in regions adjacent to the 250 and 100 μm patterns (Figure 6a, $P < 0.001$). In addition, the decrease in neuron survival in regions adjacent to the 250 and 100 μm patterns was similar (Figure 6a). Neurite density was also similar within the patterned NGF expression for widths of 250 and 100 μm, and decreased significantly in regions adjacent to the patterns (Figure 6b, $P < 0.001$). The neuronal responses observed here could be due to NGF concentration differences in the cell microenvironment caused by localized production of NGF. Importantly, decreasing the pattern width (from 250 to 100 μm) focused neurite outgrowth within the pattern to a greater extent. With 100 μm patterns of NGF expression, neurite density decreased 97% in regions directly adjacent to the pattern, significantly greater than the 70% decrease observed with 250 μm patterns (Figure 6b, $P < 0.01$). Interestingly, the primary neurite density within the pattern (250, 100 μm) was significantly higher than for neuronal co-cultures

in the absence of a pattern or for NGF added to the medium (25 ng/ml, the optimum concentration for neuron survival and neurite extension) (Figure 7, $P < 0.05$), suggesting that the patterned NGF expression provided a directional cue that increased the rate of axonal elongation and reduced aberrant sprouting. Higher ratios of pNGF to pEGFP (80:20) increased neuron survival outside the pattern, resulting in neurite extension directed toward the pattern, while lower ratios of pNGF to pEGFP (20:80) decreased neuron survival and neurite density (data not shown).

A partial differential equation model was subsequently adapted to predict concentration profiles that develop from the patterned to the unpatterned region.[45] The patterned expression of diffusible factors creates concentration gradients, with concentrations highest within the region of transfected cells and decreasing with increasing distances from the pattern (Figure 8a). The experimental results indicate that neuron survival is greatest within the pattern, corresponding to the highest NGF concentrations, and that neurite extension occurs primarily along the patterned region (Figure 6). Neurite extension has been reported to occur along stable NGF concentrations, and not down concentration gradients.[13] Consistent with these reports, neurites extend along the path of transfected cells that corresponds with the highest predicted NGF concentration. For HEK293T cells seeded on 50:50 pNGF/pEGFP immobilized complexes, an average NGF concentration of 0.4 ng/ml was predicted within the 250 μm pattern, and 0.2 ng/ml was predicted for the 100 μm pattern (Figure 8a). The lower concentration results from there being fewer transfected cells within the 100 μm pattern relative to the 250 μm pattern. Experimentally, decreasing the pattern width (from 250 to 100 μm) increased the extent to which neurites were restricted to the pattern (Figure 6b), which may result from lower neurotrophin concentrations in the region adjacent to the 100 μm pattern relative to the 250 μm pattern. The average concentration predicted within the 100 μm channel (0.2 ng/ml) was maintained for a distance of ~700 μm for the 250 μm channel. Thus, the model predicts that larger channels create higher concentrations over greater distances than narrower channels.

Mathematical modeling also predicts that increasing the rate of protein production by the cells, which could be achieved by increasing the ratio of NGF to GFP plasmid, increases the concentration within the pattern and in adjacent regions (Figure 8b and c). This mathematical prediction is consistent with the experimental results with an increasing ratio of pNGF to pGFP, where increased neuron survival was observed outside the pattern (data not shown). Interestingly, those neurons surviving outside the pattern extended neurites toward the pattern, or up the predicted concentration gradient created by the patterned transfection. In summary, the NGF concentration gradient can be modulated by the pattern dimensions and the pNGF density, and the concentration profile can be manipulated either to localize neurite growth within the pattern or to direct neurite growth toward the pattern.

Convective transport was not incorporated into the model but could be included to control the concentration gradients. If transport by convection had dominated diffusion in our experiments, the secreted NGF would have been distributed throughout the culture medium at an expected concentration of approximately 0.005 ng/ml, which does not support significant neuron survival or neurite extension. Diffusion was likely significant, enabling NGF to accumulate at the cell surface near the region of patterned transfection at concentrations (0.2–1.0 ng/ml) that promote neuron survival and neurite outgrowth. For these reasons, the localized neuron survival and neurite extension were attributed to a gradient of NGF that resulted from NGF diffusion from the pattern of expression. In terms of the *in vivo* translation of these results, morphogen gradients predicted *in vivo* have been suggested to occur mainly by diffusive mechanisms.[45] However, convective transport in conjunction with diffusion can play a role in shaping the morphogen gradients.[46]

In summary, spatial patterns of immobilized lipoplexes can produce patterns of gene expression capable of directing cellular processes. Biomaterial-based delivery of protein and DNA has been able to localize drug delivery generally to the implant site and can support the physiological processes that lead to tissue formation. However, the engineering of tissues with complex architectures will require concentrations of inductive factors to be manipulated on smaller length scales (10–100 μm) in order to direct cellular assembly and tissue formation. In this article, we have demonstrated that patterned immobilization of gene therapy vectors can regulate cellular processes on length scales of 100 μm. Patterned gene expression can potentially produce gradients of diffusible proteins for the timescales necessary to regenerate functional tissue. We have demonstrated localized neuron survival and neurite outgrowth, but a patterned gene delivery approach can be applied to many cellular responses involved in tissue regeneration, such as directed cellular migration or the patterning of stem cell differentiation that is observed in the niche. The system can be employed in fundamental studies of cellular processes and tissue formation or applied to the generation of functional tissue replacements.

MATERIALS AND METHODS

Plasmids

Plasmid DNA was purified from bacterial culture using Qiagen (Santa Clara, CA) reagents and stored in Tris-EDTA buffer at −20 °C. The plasmid pEGFPLuc has EGFP in the vector backbone with a cytomegalovirus promoter (Clontech, Mountain View, CA). The plasmid pNGF has full-length mouse NGF in the RK5 vector backbone with a cytomegalovirus promoter and was a gift from Dr. Hiroshi Nomoto (Gifu Pharmaceutical University, Japan).

Fabrication of microfluidic networks

SU8-100 negative tone photoresist (Microchem, Newton, MA) was spin-coated at 1,000 rpm for 30 seconds on silicon wafers (Ultrasil, Hayward, CA). After baking, specified regions of the photoresist were polymerized using film transparencies as the photomask (In Tandem Design, Towson, MD) and a Quintel Q-2000 mask aligner (Quintel, San Jose, CA), with UV exposure for 45 seconds. Polydimethylsiloxane, also referred to as Dow Corning Sylgard 184 Elastomer, was obtained from Krayden (Glenview, IL). Polydimethylsiloxane was cured on the photoresist molds at a 10:1 (base to curing agent) ratio at 60 °C for 5 hours. After cooling, the PDMS was peeled off the molds and ports were punched at both ends of the channels. Polydimethylsiloxane was treated with either O_2 plasma (Harrick Plasma, Ithaca, NY) for 3 minutes or soaked in a 2 mg/ml Pluronic L35 block co-polymer (gift from BASF, Mount Olive, NJ) solution in 10 mM KH_2PO_4 buffer, rinsed and dried in a sterile hood.

Complex deposition

DNA in Dulbecco's modified Eagle's medium (DMEM) (Life Technologies, Gaithersburg, MD) was complexed with Lipofectamine 2000 (Life Technologies) in DMEM (DNA to lipid, 1:1) by adding lipid to DNA and pipetting gently. Polydimethylsiloxane microchannels were reversibly sealed to TCPS wells and complexes were injected in the microchannels at the inlet port and flowed into the channel via capillary action. After 1 hour's incubation, the complexes were removed, the PDMS was peeled off, and the surfaces were rinsed twice with DMEM. For imaging deposition, plasmid DNA (pEGFPLuc) was fluorescently labeled with tetramethyl rhodamine (Mirus, Madison, WI). The deposited DNA was imaged using fluorescence microscopy, and the average complex diameter was determined using the program ImageJ.

Binding efficiency quantification

A nick translation kit (Amersham Pharmacia Biotech, Piscataway, NY) was used to radiolabel pEGFP with α-^{32}P dATP according to the manufacturer's protocol with slight modifications.

[47] Radiolabeled plasmid was complexed with Lipofectamine 2000, and a known volume of complexes was injected into PDMS microchannels sealed to TCPS. Complexes were removed after 1 hour's incubation. The PDMS was peeled away from the surface, and the surface was rinsed two times with DMEM. The TCPS, PDMS, and rinses were placed in separate scintillation vials with 10 ml Biosafe II scintillation cocktail (Research Products, Mt. Prospect, IL). Counts were determined using a scintillation counter and correlated to DNA mass using a standard curve. To normalize for the PDMS surface area PDMS to TCPS surface-area ratios were calculated as 1.5, 2, 3, and 6 for 1,000, 500, 250, and 100 μm wide channels, respectively. The binding efficiencies for each channel width were multiplied by the necessary PDMS surface area correction factor. The corrected binding efficiencies were averaged and statistically analyzed.

Patterned transfection efficiency

pEGFPLuc was complexed with Lipofectamine 2000 and incubated in the PDMS microchannels on TCPS for 1 hour. Following two DMEM rinses, HEK293T cells (ATCC, Manassas, VA) in DMEM supplemented with 10% heat-inactivated fetal bovine serum, 1% penicillin/streptomycin, and 1% sodium pyruvate were seeded on the TCPS (2.8×10^5 cells/dish) and cultured for 48 hours at 37 °C and 5% CO_2. Cells were fixed with 4% paraformaldehyde in phosphate-buffered saline and stained with 5 μg/ml Hoechst 33258 (Molecular Probes, Eugene, OR). Cells producing the EGFP (green) and cell nuclei (blue) were observed using fluorescence microscopy. The number of transfected cells was determined by counting green positive cells in five random images per pattern, and the total number of cells in each image was established by counting cell nuclei. Transfection efficiency was defined as the number of transfected cells divided by the total number of cells.

In vitro neurite outgrowth

Plasmid pNGF and pEGFPLuc were complexed with Lipofectamine 2000 at varying ratios (20:80, 50:50, and 80:20) and incubated in PDMS microchannels on TCPS as described above. The EGFP expression allowed for visualization of the patterned transfection. Following two DMEM rinses, HEK293T cells were seeded on the TCPS (8.5×10^4 cells/well). To obtain primary neurons, dorsal root ganglia were isolated from E8 white leghorn chicken eggs (Michigan State University Poultry Center, East Lansing, MI) and maintained in Hank's buffered salt solution supplemented with 6 g/l glucose until the isolation was complete. Dorsal root ganglia were incubated for 30 minutes at 37 °C in 0.25% trypsin (Worthington Biochemical, Lakewood, NJ), followed by trituration with fire-polished glass Pasteur pipettes to dissociate the ganglia. Non-neuronal and neuronal cells were separated by panning for 2 hours at 37 °C. After 8 hours' culture of the HEK293T cells, the medium was removed and the surfaces were washed with phosphate-buffered saline to remove NGF. The dissociated dorsal root ganglia neurons were seeded (5×10^4 cells/well) on the cell layer. Cells were cultured for 24 hours in complete DMEM at 37 °C and 5% CO_2. To minimize convective transport, culture dishes were not disturbed during the culture period. After the 24-hour culture, cells were fixed with 4% paraformaldehyde. The neurons were stained for the neuron-specific class III β-tubulin by incubating fixed cells in TUJ1 antibody (Covance, Berkely, CA) diluted in 5% normal goat serum (Vector Labs, Burlingame, CA) in phosphate-buffered saline for 1 hour followed by incubation in tetramethyl rhodamine isothiocyanate-conjugated goat anti-mouse secondary antibody (Jackson Immunoresearch, West Grove, PA) in phosphate-buffered saline for 30 minutes. Cells were counterstained with Hoechst 33258 to visualize cell nuclei.

Neuron survival and neurite extension

Surviving neurons were identified as those having sprouting neurites. Neurite lengths were quantified using the tracing program NeuronJ, a plugin to ImageJ.[48] Neuron survival, primary

neurite length, and total neurite length were normalized to surface areas at the pattern of transfection and distances from the pattern. Primary neurites were defined as neurites extending directly from the cell body. Neurite density was defined as total neurite length divided by the surface area. Quantifications were made from four regions of the pattern and averaged.

Mathematical modeling of concentration gradients

Mathematical modeling of NGF diffusion was used to predict the concentration profile in the culture well. Equation 1 describes one-component diffusion in two dimensions in a continuous medium with a term for protein degradation:

$$\frac{\partial C}{\partial t} = D\left[\frac{\partial^2 C}{\partial x^2} + \frac{\partial^2 C}{\partial z^2}\right] - kC, \tag{1}$$

where C is the concentration, D is the diffusivity of the protein, and k is the rate constant for protein degradation. The Crank–Nicolson implicit method was employed to solve numerically the second-order partial differential equation. The initial condition is a zero concentration throughout the culture (Equation 2). The boundary conditions indicate a flux (q), which is determined from the protein production rate, within the pattern of transfected cells (Equation 3), and no flux boundary conditions elsewhere (Equation 4–Equation 7).

$$C(x,z,t=0) = 0, \tag{2}$$

$$-D\frac{\partial C}{\partial z}\left(x<x_{\text{patt}}, z=0, t\right) = q, \tag{3}$$

$$\frac{\partial C}{\partial z}\left(x>x_{\text{patt}}, z=0, t\right) = 0, \tag{4}$$

$$\frac{\partial C}{\partial z}(x, z=z_{\max}, t) = 0, \tag{5}$$

$$\frac{\partial C}{\partial x}(x=0, z, t) = 0, \tag{6}$$

$$\frac{\partial C}{\partial x}(x=x_{\max}, z, t) = 0. \tag{7}$$

Note that the region of patterned transfection occurs within x = 0 to x_{patt}. The boundary in the x-direction ($x_{\max}$) was defined as 7.8 mm, the approximate radius of a 24-well tissue culture well. The boundary in the z-direction ($z_{\max}$) was set equal to $x_{\max}$. Values for the diffusivity of NGF and the production rate of NGF by cells transfected with the pRK5-NGF plasmid were

determined from published reports to be 12×10^{-7} cm^2/s and 1 $ng/cm^3/min$, respectively.[49, 50]

Statistics

Statistical analysis was performed using JMP software (SAS Institute, Cary, NC). Comparative analyses were executed using one-way analysis of variance with Tukey post-tests, at a 95% confidence level. Mean values with SEM are reported. All experiments were performed in triplicate.

ACKNOWLEDGMENTS

The authors thank Phil Messersmith, Stoyan Smoukov, Angela Pannier, Zain Bengali, and Laura Swift (Northwestern University) for technical assistance with plasma treatment, photolithography, and microchannel fabrication. Photolithography was performed at the Materials Processing and Crystal Growth Core Facility (Northwestern University). Financial support for this research was provided by grants from NIH (R01 GM066830, to L.D.S.) and NSF (Graduate Research Fellowship, to T.H.R.).

REFERENCES

1. Dillon R, Gadgil C, Othmer HG. Short- and long-range effects of sonic hedgehog in limb development. Proc Natl Acad Sci USA 2003;100:10152–10157. [PubMed: 12930894]
2. Marti E, Bumcrot DA, Takada R, McMahon AP. Requirement of 19K form of Sonic hedgehog for induction of distinct ventral cell types in CNS explants. Nature 1995;375:322–325. [PubMed: 7753196]
3. Briscoe J, Ericson J. The specification of neuronal identity by graded Sonic Hedgehog signalling. Semin Cell Dev Biol 1999;10:353–362. [PubMed: 10441550]
4. Liem KF Jr, Tremml G, Roelink H, Jessell TM. Dorsal differentiation of neural plate cells induced by BMP-mediated signals from epidermal ectoderm. Cell 1995;82:969–979. [PubMed: 7553857]
5. Hofmann C, Luo G, Balling R, Karsenty G. Analysis of limb patterning in BMP-7-deficient mice. Dev Genet 1996;19:43–50. [PubMed: 8792608]
6. Tickle C. Morphogen gradients in vertebrate limb development. Semin Cell Dev Biol 1999;10:345–351. [PubMed: 10441549]
7. Strigini M, Cohen SM. Wingless gradient formation in the Drosophila wing. Curr Biol 2000;10:293–300. [PubMed: 10744972]
8. Neumann CJ, Cohen SM. Long-range action of Wingless organizes the dorsal-ventral axis of the Drosophila wing. Development 1997;124:871–880. [PubMed: 9043068]
9. Zecca M, Basler K, Struhl G. Direct and long-range action of a wingless morphogen gradient. Cell 1996;87:833–844. [PubMed: 8945511]
10. Schneider IC, Haugh JM. Quantitative elucidation of a distinct spatial gradient-sensing mechanism in fibroblasts. J Cell Biol 2005;171:883–892. [PubMed: 16314431]
11. Singer AJ, Clark RA. Cutaneous wound healing. N Engl J Med 1999;341:738–746. [PubMed: 10471461]
12. Jackson CL, Reidy MA. Basic fibroblast growth factor: its role in the control of smooth muscle cell migration. Am J Pathol 1993;143:1024–1031. [PubMed: 8213998]
13. Tessier-Lavigne M, Goodman CS. The molecular biology of axon guidance. Science 1996;274:1123–1133. [PubMed: 8895455]
14. Mueller BK. Growth cone guidance: first steps towards a deeper understanding. Annu Rev Neurosci 1999;22:351–388. [PubMed: 10202543]
15. Song HJ, Poo MM. Signal transduction underlying growth cone guidance by diffusible factors. Curr Opin Neurobiol 1999;9:355–363. [PubMed: 10395576]
16. Jang JH, Houchin TL, Shea LD. Gene delivery from polymer scaffolds for tissue engineering. Expert Rev Med Devices 2004;1:127–138. [PubMed: 16293016]
17. Lutolf MP, Hubbell JA. Synthetic biomaterials as instructive extracellular microenvironments for morphogenesis in tissue engineering. Nat Biotechnol 2005;23:47–55. [PubMed: 15637621]

18. Langer R, Tirrell DA. Designing materials for biology and medicine. Nature 2004;428:487–492. [PubMed: 15057821]
19. Jang JH, Rives CB, Shea LD. Plasmid delivery in vivo from porous tissue-engineering scaffolds: transgene expression and cellular transfection. Mol Ther 2005;12:475–483. [PubMed: 15950542]
20. Shea LD, Smiley E, Bonadio J, Mooney DJ. DNA delivery from polymer matrices for tissue engineering. Nat Biotechnol 1999;17:551–554. [PubMed: 10385318]
21. Stachelek SJ, Sonq C, Alferiev I, Defelice S, Cui X, Connolly JM, et al. Localized gene delivery using antibody tethered adenovirus from polyurethane heart valve cusps and intra-aortic implants. Gene Ther 2004;11:15–24. [PubMed: 14681693]
22. Segura T, Chung PH, Shea LD. DNA delivery from hyaluronic acid-collagen hydrogels via a substrate-mediated approach. Biomaterials 2005;26:1575–1584. [PubMed: 15522759]
23. Jang JH, Bengali Z, Houchin TL, Shea LD. Surface adsorption of DNA to tissue engineering scaffolds for efficient gene delivery. J Biomed Mater Res A 2006;77A:50–58. [PubMed: 16353173]
24. Bengali Z, Pannier AK, Segura T, Anderson BC, Jang KH, Mustoe TA, et al. Gene delivery through cell culture substrate adsorbed DNA complexes. Biotechnol Bioeng 2005;90:290–302. [PubMed: 15800863]
25. Ziauddin J, Sabatini DM. Microarrays of cells expressing defined cDNAs. Nature 2001;411:107–110. [PubMed: 11333987]
26. Dertinger SK, Jiang X, Li Z, Murthy VN, Whitesides GM. Gradients of substrate-bound laminin orient axonal specification of neurons. Proc Natl Acad Sci USA 2002;99:12542–12547. [PubMed: 12237407]
27. Gunawan RC, Choban ER, Conour JE, Silvestre J, Schook LB, Gaskins HR, et al. Regiospecific control of protein expression in cells cultured on two-component counter gradients of extracellular matrix proteins. Langmuir 2005;21:3061–3068. [PubMed: 15779985]
28. Luo Y, Shoichet MS. A photolabile hydrogel for guided three-dimensional cell growth and migration. Nat Mater 2004;3:249–253. [PubMed: 15034559]
29. Adams DN, Kao EY, Hypolite CL, Distefano MD, Hu WS, Letourneau PC. Growth cones turn and migrate up an immobilized gradient of the laminin IKVAV peptide. J Neurobiol 2005;62:134–147. [PubMed: 15452851]
30. DeLong SA, Moon JJ, West JL. Covalently immobilized gradients of bFGF on hydrogel scaffolds for directed cell migration. Biomaterials 2005;26:3227–3234. [PubMed: 15603817]
31. Vepari CP, Kaplan DL. Covalently immobilized enzyme gradients within three-dimensional porous scaffolds. Biotechnol Bioeng 2006;93:1130–1137. [PubMed: 16444737]
32. Whitesides GM, Ostuni E, Takayama S, Jiang X, Ingber DE. Soft lithography in biology and biochemistry. Annu Rev Biomed Eng 2001;3:335–373. [PubMed: 11447067]
33. Xia YN, Whitesides GM. Soft lithography. Annu Rev Mater Sci 1998;28:153–184.
34. Papra A, Bernard A, Juncker D, Larsen NB, Michel B, Delamarche E. Microfluidic networks made of poly(dimethylsiloxane), Si, and Au coated with polyethylene glycol for patterning proteins onto surfaces. Langmuir 2001;17:4090–4095.
35. McDonald JC, Duffy DC, Anderson JR, Chiu DT, Wu H, Schueller OJ, et al. Fabrication of microfluidic systems in poly(dimethylsiloxane). Electrophoresis 2000;21:27–40. [PubMed: 10634468]
36. Lee S, Iten R, Muller M, Spencer ND. Influence of molecular architecture on the adsorption of poly (ethylene oxide)-poly(propylene oxide)-poly(ethylene oxide) on PDMS surfaces and implications for aqueous lubrication. Macromolecules 2004;37:8349–8356.
37. Liu F, Yang JP, Huang L, Liu DX. Effect of non-ionic surfactants on the formation of DNA/emulsion complexes and emulsion-mediated gene transfer. Pharm Res 1996;13:1642–1646. [PubMed: 8956328]
38. Gebhart CL, Sriadibhatla S, Vinogradov S, Lemieux P, Alakhov V, Kabanov AV. Design and formulation of polyplexes based on pluronic-polyethyleneimine conjugates for gene transfer. Bioconjug Chem 2002;13:937–944. [PubMed: 12236774]
39. Nguyen HK, Lemieux P, Vinogradov SV, Gebhart CL, Guerin N, Paradis G, et al. Evaluation of polyether-polyethyleneimine graft copolymers as gene transfer agents. Gene Ther 2000;7:126–138. [PubMed: 10673718]

40. Pannier AK, Anderson BC, Shea LD. Substrate-mediated delivery from self-assembled monolayers: effect of surface ionization, hydrophilicity, and patterning. Acta Biomater 2005;1:511–522. [PubMed: 16701831]
41. Miller C, Shanks H, Witt A, Rutkowski G, Mallapragada S. Oriented Schwann cell growth on micropatterned biodegradable polymer substrates. Biomaterials 2001;22:1263–1269. [PubMed: 11336298]
42. Kam L, Shain W, Turner JN, Bizios R. Axonal outgrowth of hippocampal neurons on micro-scale networks of polylysine-conjugated laminin. Biomaterials 2001;22:1049–1054. [PubMed: 11352086]
43. Miller C, Jeftinija S, Mallapragada S. Synergistic effects of physical and chemical guidance cues on neurite alignment and outgrowth on biodegradable polymer substrates. Tissue Eng 2002;8:367–378. [PubMed: 12167224]
44. Heller DA, Garga V, Kelleher KJ, Lee TC, Mahbubani S, Sigworth LA, et al. Patterned networks of mouse hippocampal neurons on peptide-coated gold surfaces. Biomaterials 2005;26:883–889. [PubMed: 15353199]
45. Lander AD, Nie Q, Wan FY. Do morphogen gradients arise by diffusion? Dev Cell 2002;2:785–796. [PubMed: 12062090]
46. Helm CL, Fleury ME, Zisch AH, Boschetti F, Swartz MA. Synergy between interstitial flow and VEGF directs capillary morphogenesis in vitro through a gradient amplification mechanism. Proc Natl Acad Sci USA 2005;102:15779–15784. [PubMed: 16249343]
47. Segura T, Volk MJ, Shea LD. Substrate-mediated DNA delivery: role of the cationic polymer structure and extent of modification. J Control Release 2003;93:69–84. [PubMed: 14602423]
48. Meijering E, Jacob M, Sarria JCF, Steiner P, Hirling H, Unser M. Design and validation of a tool for neurite tracing and analysis in fluorescence microscopy images. Cytometry A 2004;58A:167–176. [PubMed: 15057970]
49. Stroh M, Zipfel WR, Williams RM, Webb WW, Saltzman WM. Diffusion of nerve growth factor in rat striatum as determined by multiphoton microscopy. Biophys J 2003;85:581–588. [PubMed: 12829512]
50. Whittlesey KJ, Shea LD. Nerve growth factor expression by PLG-mediated lipofection. Biomaterials 2006;27:2477–2486. [PubMed: 16316681]

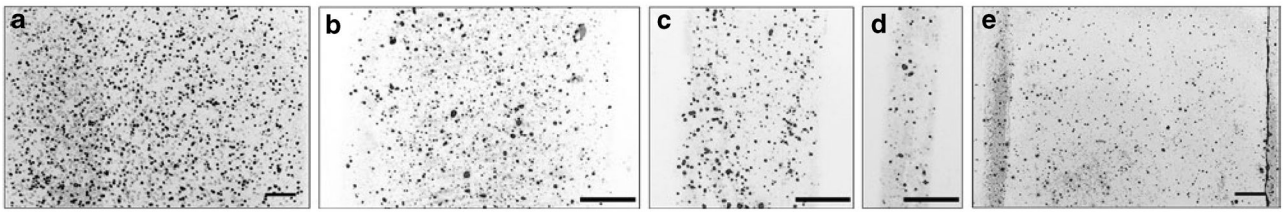

Figure 1. Patterned lipoplex deposition

Immobilized lipoplexes (red) deposited in Pluronic-treated polydimethylsiloxane microchannels: (**a**) 1,000 μm, (**b**) 500 μm, (**c**) 250 μm, and (**d**) 100 μm. (**e**) Lipoplexes deposited using untreated microchannels (1,000 μm). Bars = 100 μm.

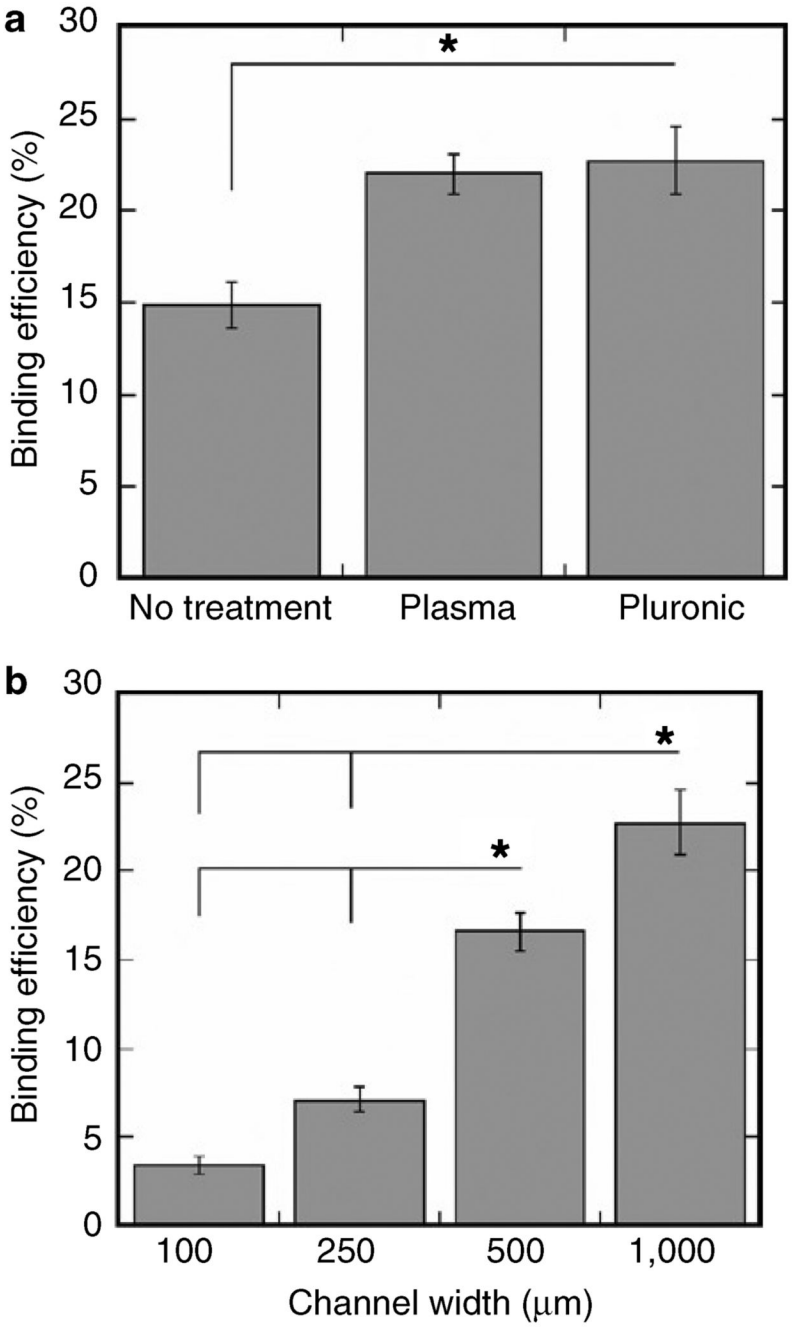

Figure 2. Patterned lipoplex binding efficiency

Quantification of lipoplex binding efficiency (total bound divided by total incubated in the channel) using polydimethylsiloxane microchannels, while varying (**a**) channel treatments (no treatment, O_2 plasma, Pluronic) and (**b**) channel widths (100, 250, 500, 1,000 μm). Values are reported as mean ± SEM (* $P < 0.05$).

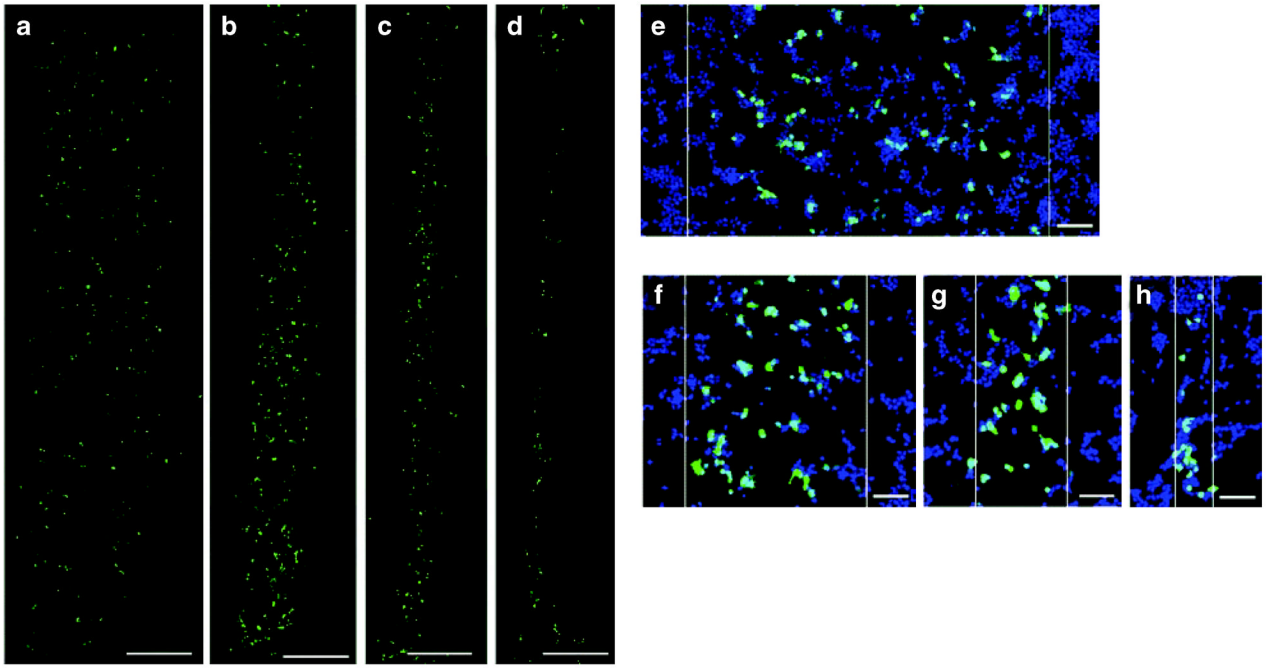

Figure 3. HEK293T cells expressing the reporter gene enhanced green fluorescent protein (EGFP) in a pattern

EGFP expression (green) within cells cultured on substrates with patterned DNA complex deposition using Pluronic-treated microchannels: (**a**) 1,000 μm, (**b**) 500 μm, (**c**) 250 μm, and (**d**) 100 μm. Higher-magnification images present cell nuclei (blue) and transfected cells (green) overlaid: (**e**) 1,000 μm, (**f**) 500 μm, (**g**) 250 μm, and (**h**) 100 μm. White lines indicate pattern boundaries. Bars = 500 μm (**a–d**) and 100 μm (**e–h**).

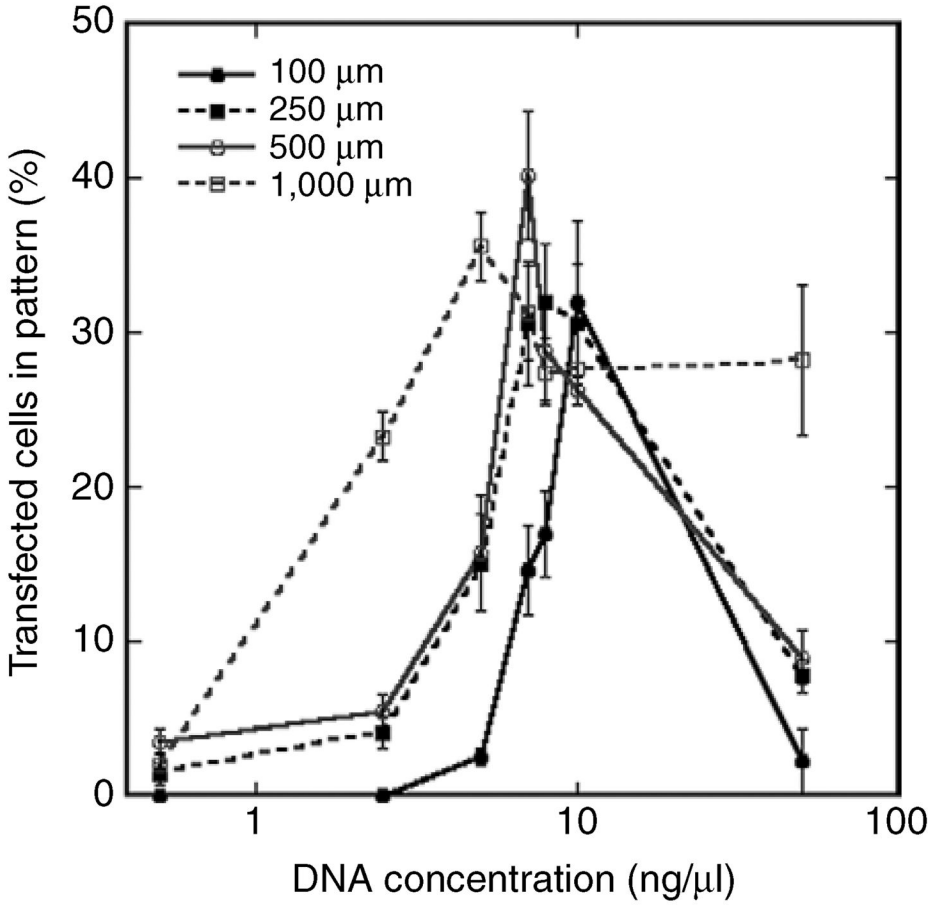

Figure 4. Transfection efficiency was dependent on microchannel width and vector concentration

Transfection efficiency (percentage of transfected cells) in the pattern as a function of vector concentration and channel width. Lipoplex deposition was performed within Pluronic-treated microchannels. Values are reported as mean ± SEM.

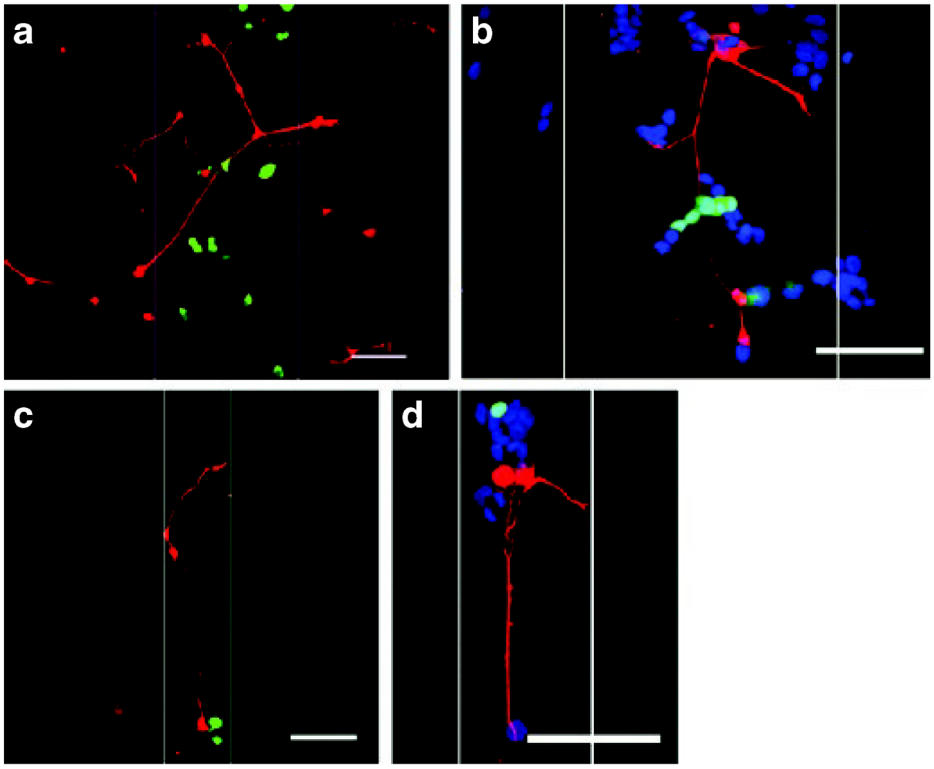

Figure 5. Neurons cultured with cells expressing nerve growth factor (NGF) in patterns

Neurite extension (red) was observed at the region of transfected cells (green): (**a**, **b**) 250 μm width; (**c**, **d**) 100 μm width. pNGF to pEGFP ratio of 50:50. White lines indicate pattern boundaries. Cell nuclei (blue) are visible in (**b**, **d**). Bars = 100 μm.

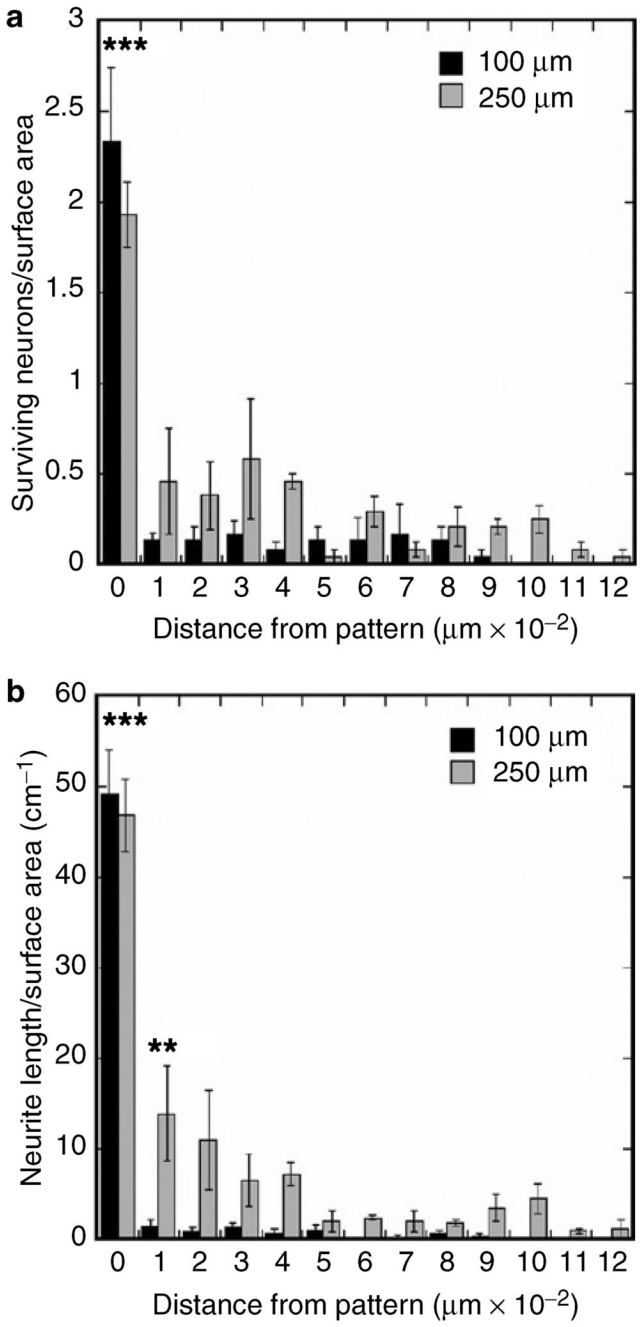

Figure 6. Neuron survival and neurite outgrowth primarily observed within patterns of nerve growth factor (NGF) expression

(**a**) Neuron survival, normalized to surface area; (**b**) total neurite density quantified within and outside the region of patterned expression. Values are reported as mean ± SEM (** $P < 0.01$, *** $P < 0.001$).

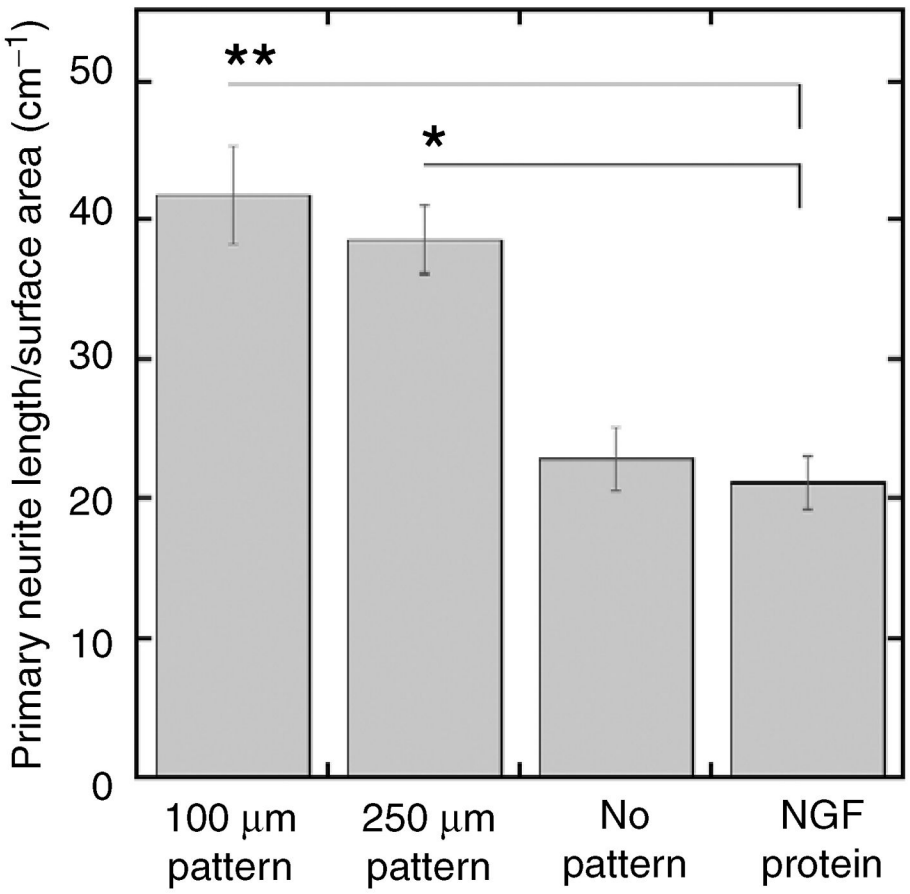

Figure 7. Primary neurite density on patterned nerve growth factor (NGF) expression and non-patterned controls

The primary neurite density was greater on patterns of NGF expression than for cultures with NGF expression and no pattern or cultures with NGF added to the media. Values are reported as mean ± SEM (* $P < 0.05$, ** $P < 0.01$).

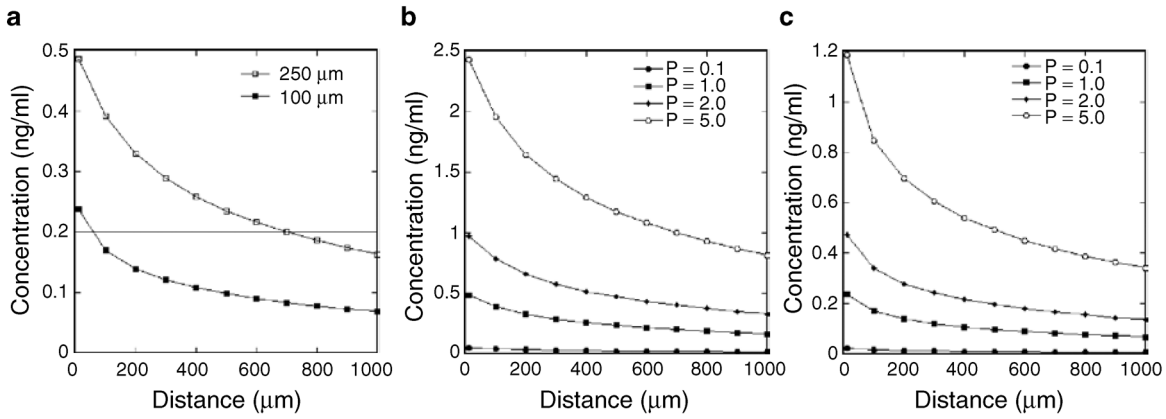

Figure 8. Predicted nerve growth factor (NGF) concentration gradients

(**a**) Mathematical model predictions of the NGF concentration profile for channels with widths of 250 and 100 μm. Note that the kinetic constant describing the rate of protein production (p) was estimated to be 1 ng/cm^3/min. The production rate was varied and the concentrations modeled for (**b**) 250 and (**c**) 100 μm wide patterns. Gradients were modeled for 24 hours, and the reported concentrations are those at the material surface ($z = 0$).